



The influence of fumed silica content, dispersion energy, and humidity on the stability of shear thickening fluids

Daniel Alves Heinze¹ · Danilo Justino Carastan¹

Received: 16 January 2020 / Revised: 3 April 2020 / Accepted: 19 May 2020 / Published online: 28 May 2020
© Springer-Verlag GmbH Germany, part of Springer Nature 2020

Abstract

Shear thickening fluids (STFs) are smart materials that change from liquid to solid reversibly when undergoing critical stresses. These materials are good alternatives to improve applications where energy dissipation is important, for example, in the fabrication of liquid body armor and shock absorbing protective gear. However, as much as it is known about the effect of several variables on their properties, such as particle concentration and medium viscosity, the stability of these colloidal dispersions over time and over shearing is not yet well understood. The development and design of new applications depend on predicting for how long the material will keep its properties. In this project, we studied the influence of fumed silica content, ultrasonication energy used during dispersion of the silica particles, and humidity during storage to analyze the changes in properties of STFs. The influence of shearing magnitude on their properties was also studied. STFs with higher amounts of silica and produced using less dispersion energy showed the highest viscosity peak on initial tests, but they were also the least stable over time, due to flocculation of the particles. In stable samples, water absorption led to a large loss of maximum viscosity. The presence of humidity on samples diminished the overall viscosity, but did not prevent the sample from becoming a gel if the parameters used resulted in an unstable STF. Shearing the STF reduced its maximum viscosity, being more evident in samples with higher viscosity.

Keywords Shear thickening fluids · Stability · Fumed silica · PEG · Rheology · Ultra-sonication

Introduction

Shear thickening fluids (STFs) are smart materials that show a steep increase in viscosity when undergoing critical shear rates. This discontinuous, nonlinear increase in viscosity elevates the energy required for the material to flow, causing it to change its apparent behavior from a liquid to a solid, reversibly (Barnes 1989; Mewis and Wagner 2012). STFs are generally obtained from concentrated colloidal suspensions. The shear thickening phenomenon was initially considered a problem in industrial processes where variations in the shear rate in the fluid caused by equipment or variations in pipe diameter resulted in increased fluid viscosity, jamming pipes, and

breaking equipment (Barnes 1989). It was later observed that this increase in the viscosity of the fluid results in good energy dissipation properties. Thus, several studies began to be developed where energy dissipation plays a fundamental role using STFs. Most studies started testing properties of Kevlar fibers impregnated with STF, such as resistance to bullet and stab penetration and impact dissipation in body armor. One of the big advantages of using STFs in Kevlar body armor is that it can obtain the same or better properties than neat Kevlar, but using fewer layers of fabric, resulting in lighter and more flexible vests (Lee et al. 2003; Egres et al. 2005; Song et al. 2011; Lee et al., 2013; Khalili et al. 2015; Gürgen and Kuşhan 2017). Different explanations have been proposed on why discontinuous shear thickening (DST) occurs. One of the first models proposed an order-disorder transition in the particles. In this model, as external stresses are applied, the particles rearrange, generating normal stresses through the fluid, causing the material to exhibit a rigid behavior and resulting in an abrupt increase in viscosity (Hoffman 1972, 1974, 1982, 1998; Mewis and Wagner 2012). Later, it was shown that this phenomenon may occur, but it is not exclusively necessary for

✉ Danilo Justino Carastan
danilo.carastan@ufabc.edu.br

Daniel Alves Heinze
daniel.heinze92@gmail.com

¹ Engineering, Modeling and Applied Social Sciences Center (CECS), Federal University of ABC, São Paulo 09210-580, Brazil

DST. Another famous model is about the formation of hydroclusters, where shearing would provide enough energy to overcome the repulsion between particles, approximating them and hindering the flux of the material (Bossis 1985). A third theory is called dilatancy, where the increase in viscosity is compared to that in granular materials, where they show an increase in volume when sheared. In an STF, this increase in volume would hinder the movement of particles and increase the viscosity of the material (Reynolds 1885; Metzner and Whitlock 1958). Although several models have been proposed, it does not mean they are excluding and that only one could be happening.

Many variables are known to influence STFs, playing important parts in their final properties and stability. First, particle-particle interaction is one of the properties that play a major role in their rheological behavior. When continuous shear thickening behavior was discovered, the phenomenon was described as occurring only in deflocculated suspensions, and the slightest attraction between particles would be enough to eliminate and avoid the appearance of the phenomenon (Freundlich and Jones 1936). Thus, particles must be repulsive or neutral to each other (Freundlich and Jones 1936; Barnes 1989; Bles 2002). In these deflocculated particle systems, the material will have low viscosity at rest or low shear, with a little shear thinning behavior. For high shear rates, it exhibits shear thickening behavior, reaching high viscosity values depending on the type and amount of particles. This type of system has little or no sedimentation at rest. On the other hand, flocculated systems tend to form larger particles, resulting in higher viscosities at low shear rates, but with a strong shear thinning behavior as the rate increases. In addition, flocculated systems tend to settle when at rest (Barnes 1989; Hunter 2001; Bles 2002). Another important factor in dispersion stability is the type of medium where the particles are dispersed. Solvents that have good interaction with the particles tend to facilitate their stabilization, avoiding flocculation. This is seen in the case of silica as a dispersed particle. In solvents that allow the dissociation of silanols on the silica surface, such as water and ethylene glycol, an electrostatic charge layer naturally occurs, stabilizing the particles (Laskowski and Kitchener 1969; Bles 2002). This was shown by Laskowski in 1969, where by modifying the surface of hydrophilic silica to hydrophobic through the addition of methyl groups, the suspension no longer exhibited shear thickening behavior, forming a gel even at low concentrations of modified silica (Laskowski and Kitchener 1969).

As to the properties of the STF, increasing particle volume results in higher viscosity of the material. This is seen at low shear rates, but mainly at the peak viscosity due to DST behavior. The viscosity increase with increasing volume fraction occurs until it reaches a maximum limit where the dispersion becomes solid-like. This upper limit depends on the characteristics of the particles and the medium in which they are

dispersed. In addition to the increase in viscosity, the increase in particle concentration results in a decrease in the critical shear rate for DST to occur (Barnes 1989; Bertrand et al. 2002; Cao et al. 2018). As well as the particle volume fraction, increasing the average particle size decreases the critical shear rate for the DST to happen (Barnes 1989; Maranzano and Wagner 2001). However, it is important to note that very large particles, usually those that do not exhibit colloidal behavior, tend to sediment and mask the dilating properties of the fluid (Metzner and Whitlock 1958; Brown et al. 2010; Brown and Jaeger 2012).

Regarding the geometry of the particles, it is experimentally observed that anisotropic particles tend to exhibit shear thickening behavior at lower volume fractions. This is the case of fumed silica, which presents aggregates with irregular 3D geometry (Barthel et al. 2008). STFs produced with this type of silica usually have a shear thickening peak at volume fractions as low as 10–15 vol%, in contrast to 50–60 vol% for spherical silica particles (Raghavan and Khan 1997; Raghavan et al. 2000; Negi and Osuji 2009).

Besides particle aspects, the continuous phase in an STF also contributes to its final properties. As most of the composition of an STF is the liquid phase, increasing its viscosity results in an increase in the total viscosity of the system. Generally, the stability of a suspension tends to be favored by increasing the viscosity of the continuous phase, as it hinders particle mobility and minimizes the tendency to agglomerate. However, for a silica-PEG STF, larger molar masses of the continuous phase imply longer polymer chains, resulting in fewer hydroxyl terminal groups, which are mainly responsible for bonding with silanols on the silica surface, stabilizing the suspension. Thus, a higher viscosity polyethylene glycol may lead to destabilization of the suspension under certain conditions (Hoffman 1982; Liu et al. 2015).

Concerning the effects of temperature on the properties of STFs, its impacts are primarily associated with continuous phase modifications and are reversible, as in an increase/decrease in viscosity caused by temperature (Barnes 1989; Warren et al. 2015). However, permanent changes in the fumed silica-PEG STF may also occur upon heating, because of changes in particle-particle interactions. What is seen is that for certain particle volume fractions, heating the STF above 45 °C decreases the amount of hydrogen bonding between PEG and silica. Silica particles tend to make fewer PEG bonds and more bonds between themselves with increasing temperature. The result is the formation of a three-dimensional network between the silica particles, leading to irreversible gelation of the suspension. The explanation for this is that with increasing temperature, there is a weakening of hydrogen bonds between the particle and the solvent, as well as increased particle mobility by Brownian motion and decreased bonding strength of the solvation layer, which prevents the particles to bond and keep them stable. This phenomenon

Table 1 Silica compositions used to prepare shear thickening fluids

Ethanol mL	Silica A200		PEG 300 Volume fraction
	Mass fraction	Volume fraction	
18.000	0.165	0.100	0.900
18.000	0.195	0.120	0.880
18.000	0.225	0.140	0.860

was most commonly seen with the increase in particle volume fraction and was not observed at concentrations close to 10 vol% of fumed silica particles. The decrease in PEG molar mass also favored the suspension stability with increasing temperature, as it increases the number of hydroxyls present, which stabilizes the silica (Liu et al. 2015).

All those aspects presented have a big impact on the properties and stability of STFs, being crucial when designing the smart material. However, another important aspect to consider about STFs is their time stability and the influence of humidity in their properties. Soutrenon et al. reported that STFs of monodisperse silica particles tend to lose their DST behavior when they are stored in a chamber with 100% of relative humidity over 15 days, leading to a loss of overall viscosity, whereas being stored in a desiccator resulted in the loss of DST with an increase in viscosity at low shear rates and a shear thinning behavior (Soutrenon et al. 2013). They also reported the influence of temperature on the storage of the material over 15 and 45 days, indicating that the properties of STFs are better retained if stored at freezing temperatures. However, no detailed studies have been published regarding the stability of STFs over time when related to the composition of the material, as well as how humidity and shearing decreases the stability of fumed silica STFs. In this study, we focus on studying the influence of fumed silica content, dispersion energy, and humidity on the stability of shear thickening fluids over a period of 16 weeks, with samples stored in regular and low humidity environments. We also investigate how shearing the STF impact its properties as well.

Materials and methods

Aerosil A200 fumed silica was supplied by Evonik with average surface area of 200 m²/g. These particles are mainly

spherical with sizes between 5 and 50 nm, but during their processing, due to the use of high temperatures, they aggregate, forming branched chains with sizes between 100 and 500 nm (Barthel et al. 2008). Polyethylene glycol 300 (PEG 300) obtained from Nox Solutions (Brazil) with average molecular weight of 300 g/mol was used as the continuous phase. PEG 300 is an oligomer with low molecular weight, resulting in a higher number of hydroxyls available, 367 mg KOH/g in average. Ethanol 99.5% was obtained from Nox Solutions (Brazil) and used as received.

Silica was dried for 24 h at 70 °C prior to use. Samples were prepared following the compositions in Table 1.

Studies have shown that good shear thickening properties can be attained at a fumed silica content of around 20 wt.% (Feng et al. 2014; Gürgen et al. 2016; Gürgen and Kuşhan 2017; Chatterjee et al. 2019; Singh et al. 2019). Previous results obtained by our group of samples produced using the processing parameters described below confirmed that a weight fraction of silica smaller than 16.5% did not result in shear thickening fluids, while samples with a fraction higher than 22.5 wt.% resulted in a solid-like gel instead of a fluid.

Fumed silica tends to form secondary bonds and agglomerates; therefore, the particles must be properly dispersed in the liquid medium. To facilitate dispersion, 3 mL of ethanol was added for each 1 mL of PEG + silica mixture. Each composition in Table 1 was dispersed using a 20 kHz Sonics Vibracell VCX 750 ultrasonic probe that has a maximum oscillation amplitude of 114 µm. Probe sonication is a type of direct ultrasonication that makes use of the cavitation phenomenon, where pressure variations form bubbles that implode, delivering high amounts of energy to the sample, being a good option to disperse nanoparticles (Gedanken 2003; Birkin et al. 2005; Taurozzi et al. 2011). Ultrasonication parameters used are shown in Table 2.

Our previous results showed that sonicating a sample for 30 min using a probe amplitude of 20%, totaling around 10 kJ of energy, did not deliver enough energy to disperse the particles and obtain a fluid, resulting in a gel. Amplitudes of 60% or higher led to the intense formation of big bubbles during sonication, decreasing the energy transferred to the sample, not forming a fluid either. The literature also reports that 40% of amplitude works well for fumed silica (Singh et al. 2019). Thus, probe amplitudes within the range of 30 to 50% were chosen for sample preparation. After dispersion, samples were kept in an oven for 24 h at 70 °C to make the ethanol

Table 2 Ultrasonication parameters used to disperse silica nanoparticles in PEG

Time (min)	Probe amplitude (%)	Amplitude oscillation (µm)	Energy delivered (kJ)
30	30	34.2	25.0
30	40	45.6	40.0
30	50	57.0	55.0

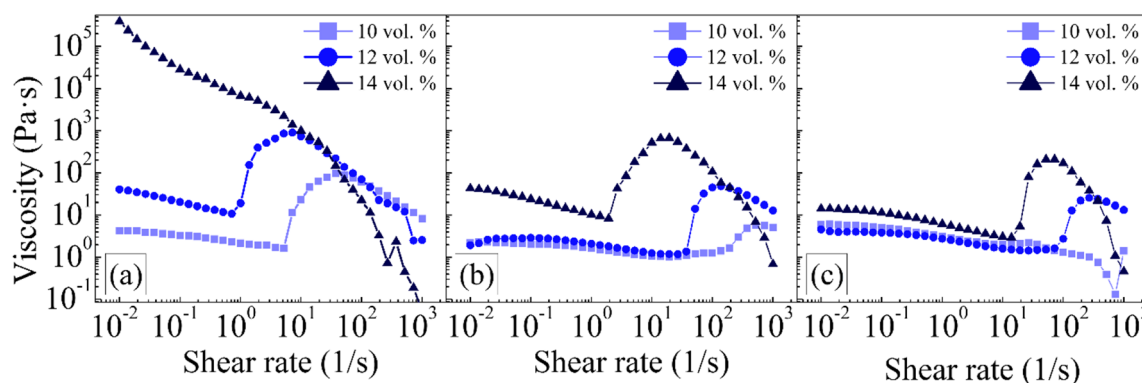


Fig. 1 Viscosity as a function of shear rate for samples with 10, 12, and 14 vol% of silica produced using probe amplitude of **a** 30%, **b** 40%, and **c** 50%

evaporate. Fourier transform infrared spectroscopy (FTIR) was used to confirm that all ethanol had been evaporated.

Rheological characterization was performed using an MCR 502 Anton-Paar rheometer with a 25 mm parallel-plate geometry and gap between plates of 1 mm. The viscosity was measured at 25 °C as a function of shear rate from 0.01 to 1000 s⁻¹. Prior to the viscosity sweep, samples were sheared for 60 s at 1 s⁻¹ and then rested for 60 s, in order to eliminate shearing history and prevent the formation of weak physical gels. The viscosity sweep consisted of 36 points in a logarithmic ramp with a density of 7 points per decade. The duration at each point also followed a logarithmic ramp, starting at 100 s and ending at 0.5 s, resulting in a total of 708.8 s for the viscosity sweep. Fresh samples were initially tested 2 h after leaving the oven (labeled as week 0), and then, each sample had its volume divided in two parts. One of them was stored in a desiccator, in order to avoid humidity absorption, while the other half remained open in room conditions, with humidity of 45 ± 10%. The temperature was kept at 23 ± 3 °C for both cases and they were stored in the absence of light. Tests were carried out after 2, 4, 8, 12, and 16 weeks to study the stability of the STFs over time and the influence of water absorption in their properties. All samples were prepared at least in duplicate.

Water content was measured using a thermogravimetric analyzer (TGA) Q5000 IR from TA instruments, with temperature varying from 27 to 600 °C with a heating ramp of 10 °C/min. Sample images were obtained using a field emission scanning electron microscope (FESEM) JMS-6701F

from Jeol, with accelerating voltage of 5.0 kV. For each image taken, the area of 100 particles was measured using the software ImageJ. Each particle had its perimeter marked and the area was calculated by the software. Smaller aggregate sizes were also measured in water using a dynamic light scattering (DLS) device Zetasizer NanoZS, from Malvern Panalytical, with optical path length of 10 mm and measurement angle of 173°, at a temperature of 25 °C. Results were obtained from the average of 50 sweeps of 12 s each. DLS was able to measure particle sizes between 1 and 1000 nm.

Results and discussion

Rheological characterization of samples in week 0 showed that increasing the fraction of silica resulted in an increase in the critical viscosity of the samples and in a lower critical shear rate for the DST to happen. These results have been extensively reported in the literature (Barthel et al. 2008; Feng et al. 2014; Gürgen et al. 2016; Gürgen and Kuşhan 2017; Chatterjee et al. 2019). Also, the same behavior was seen when decreasing probe amplitude, because less energy was delivered to the sample, resulting in bigger particle agglomerates, which leads to higher critical viscosity (Barnes 1989). Viscosity as a function of shear rate for all compositions at different probe amplitudes can be seen in Fig. 1, and the values of critical viscosity and critical shear rate of these samples are shown in Table 3.

Table 3 Critical viscosity (η_c) and critical shear rate ($\dot{\gamma}_c$) as a function of volume fraction of silica and probe amplitude

Amplitude (%)	10 vol%		12 vol%		14 vol%	
	η_c (Pa.s)	$\dot{\gamma}_c$ (1/s)	η_c (Pa.s)	$\dot{\gamma}_c$ (1/s)	η_c (Pa.s)	$\dot{\gamma}_c$ (1/s)
30	96.1	7.2	902.3	1.4	–	–
40	5.71	268.0	48.23	51.8	673.32	2.7
50	–	–	25.39	139.0	210.47	19.3

Table 4 Viscosity increase ratio (η_c/η_{ons}) for the samples tested in week 0

Amplitude (%)	Viscosity increase ratio- η_c/η_{ons}		
	10 vol%	12 vol%	14 vol%
30	57.98	83.83	–
40	5.55	40.87	80.88
50	–	17.68	72.12

The most extreme processing conditions tested did not result in shear thickening fluids. Using probe amplitude of 30% in a sample with 14% of silica resulted in a gel, where the maximum viscosity is seen at rest, with a decrease in viscosity when increasing shear rate. This is a result of inadequate dispersion of the silica, causing particles to flocculate (Barnes 1989). In the opposite case of 10% of silica dispersed with 50% of probe amplitude, the size of the agglomerates after dispersion was not enough for the shear thickening behavior to occur, due to the excessive energy transferred to a small fraction of particles. Thus, from an initial perspective, a sample with 12% of silica and 30% of amplitude has the highest critical viscosity. This sample is also one with the highest viscosity increase ratios (critical viscosity/viscosity at the onset of shear thickening: η_c/η_{ons}), as seen in Table 4.

The stability of the samples was studied within a period of up to 16 weeks. Viscosity curves as a function of time of STF's

prepared with probe amplitude of 30% are shown in Fig. 2, for samples with 10 and 12% of silica.

Using 30% of probe amplitude led to the highest critical viscosity among the tested samples, but it also led to instability of the STF. Samples with 10% of silica produced using 30% of amplitude did not show shear thickening behavior after the initial tests when stored in a low humidity environment, or past 2 weeks, when stored in a regular humidity environment. Also, the viscosity of samples in the absence of humidity was much higher. When using 12% of silica, no storage condition granted an STF past the initial test, all samples were quickly transformed into gels. The same happened with samples with 14% of silica, except they became hard solids past week 0, and thus could not be tested in the rheometer. Table 5 presents the critical viscosity, viscosity increase ratio, and critical shear rate of samples on their last stable test as STF's.

The stability of shear thickening fluids produced using 40% of probe amplitude is shown in Fig. 3 for samples with 10, 12, and 14 vol% of silica.

The higher energy delivered to the samples during ultrasonication decreased the critical viscosity, but it also led to higher stability of the samples, mainly when stored in a low humidity environment. Samples with 10% of silica produced using 40% of probe amplitude showed a small critical viscosity on week 0, but when it was kept in a dry environment, the critical viscosity increased from 5.71 Pa.s in week 0 to 131.30 Pa.s in week 16 and remained stable throughout 16 weeks. Most of the changes in sample properties happened during the first 4 weeks. When stored in a regular humidity

Fig. 2 Viscosity as a function of shear rate of samples with different silica content processed with 30% of probe amplitude after 2, 4, 8, 12, and 16 weeks. **a** 10 vol% regular humidity, **b** 10 vol% low humidity, **c** 12 vol% regular humidity, **d** 12 vol% low humidity

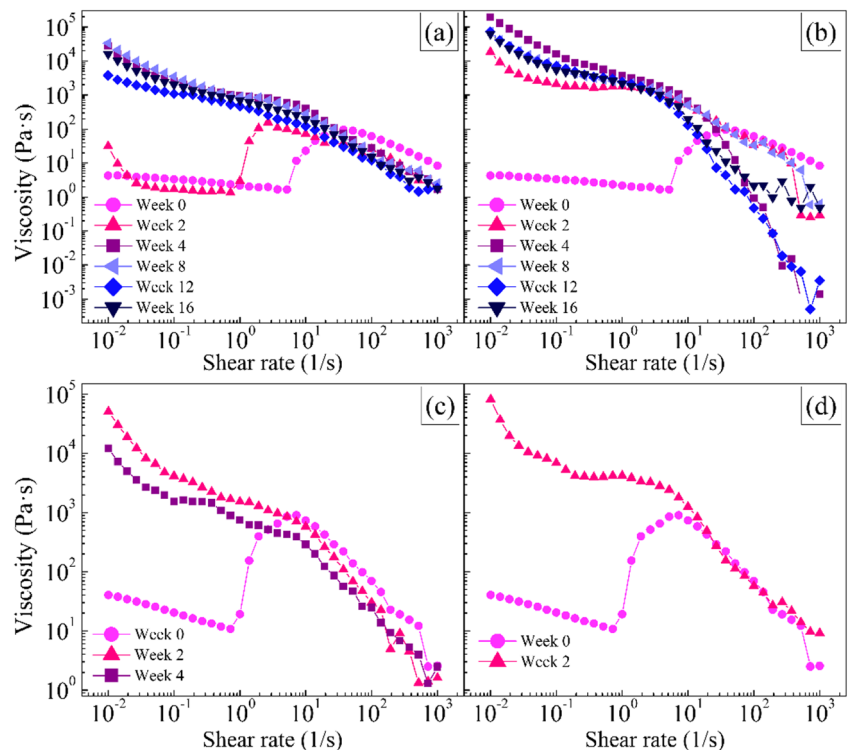


Table 5 Critical viscosity (η_c), viscosity increase ratio (η_c/η_{ons}), and critical shear rate ($\dot{\gamma}_c$) of the samples prepared with probe amplitude of 30% in the last week where they behaved as stable STFs (w_s)

Volume fraction of silica (%)	Regular humidity				Low humidity			
	w_s	η_c (Pa.s)	η_c/η_{ons}	$\dot{\gamma}_c$ (1/s)	w_s	η_c (Pa.s)	η_c/η_{ons}	$\dot{\gamma}_c$ (1/s)
10	2	157.31	116.32	1.39	0	—	—	—
12	0	—	—	—	0	—	—	—
14	—	—	—	—	—	—	—	—

environment, overall viscosity fell, although there is still a small peak of viscosity. Increasing the amount of silica resulted in greater instability independently on the presence of water. Samples with 12% of silica showed a shear thickening

behavior for 2 weeks, while those with 14% showed the same behavior only for the initial tests. Overall viscosity remained low when in the presence of humidity for all samples. Table 6 summarizes the critical viscosity, viscosity increase ratio, and

Fig. 3 Viscosity as a function of shear rate of samples with different silica content processed with 40% of probe amplitude after 2, 4, 8, 12, and 16 weeks. **a** 10 vol% regular humidity, **b** 10 vol% low humidity, **c** 12 vol% regular humidity, **d** 12 vol% low humidity, **e** 14 vol% regular humidity, **f** 14 vol% low humidity

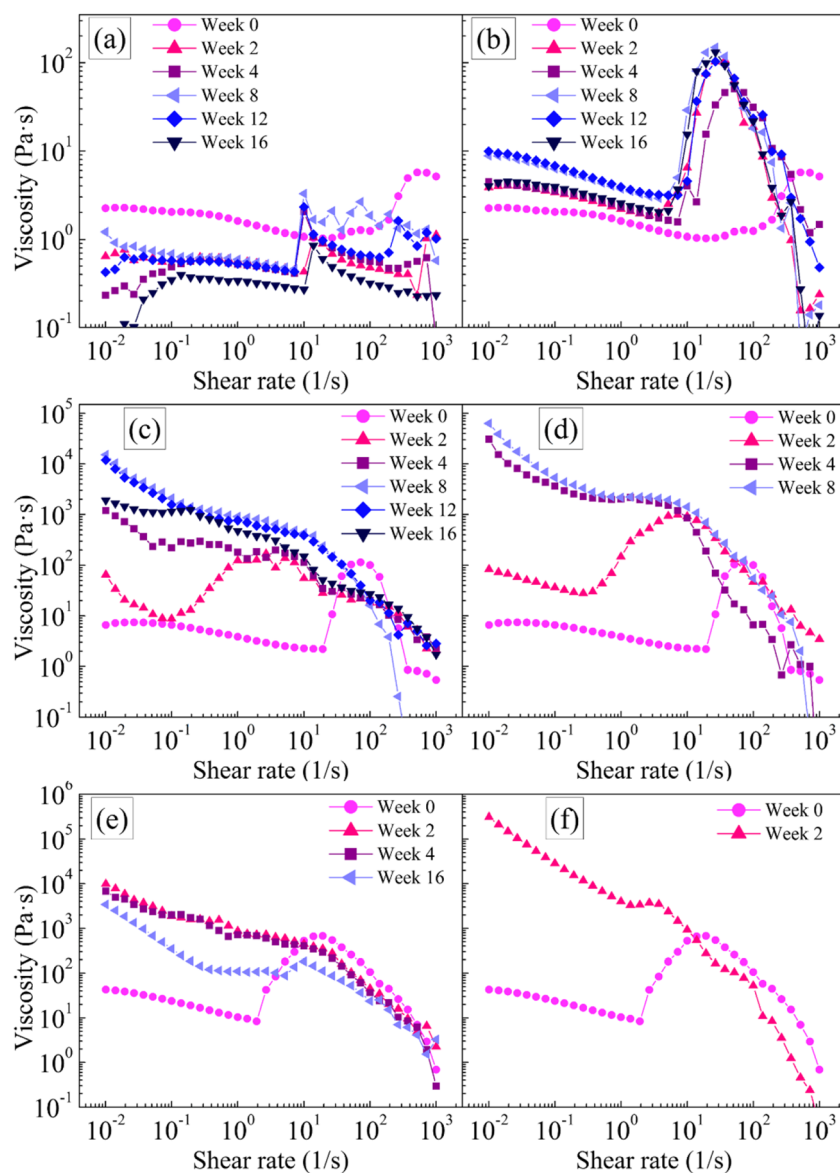


Table 6 Critical viscosity (η_c), viscosity increase ratio (η_c/η_{ons}), and critical shear rate ($\dot{\gamma}_c$) of the samples prepared with probe amplitude of 40% in the last week where they behaved as stable STF's (w_s)

Volume fraction of silica (%)	Regular humidity				Low humidity			
	w_s	η_c (Pa.s)	η_c/η_{ons}	$\dot{\gamma}_c$ (1/s)	w_s	η_c (Pa.s)	η_c/η_{ons}	$\dot{\gamma}_c$ (1/s)
10	16	0.85	14.97	13.90	16	131.30	64.73	7.20
12	2	169.06	19.49	0.14	2	971.58	35.03	0.37
14	0	–	–	–	0	–	–	–

critical shear rate of samples prepared using 40% of amplitude.

The last ultrasonication condition tested was 50% of probe amplitude. Viscosity as a function of time for samples produced using 10, 12, and 14% of silica is shown in Fig. 4.

Increasing further the dispersion energy resulted in samples with even smaller critical viscosity. Freshly prepared samples containing 10% of silica did not exhibit shear thickening behavior, but similarly to the samples prepared using 40% of amplitude, shear thickening behavior starts to slowly appear

Fig. 4 Viscosity as a function of shear rate of samples with different silica content processed with 50% of probe amplitude after 2, 4, 8, 12, and 16 weeks. **a** 10 vol% regular humidity, **b** 10 vol% low humidity, **c** 12 vol% regular humidity, **d** 12 vol% low humidity, **e** 14 vol% regular humidity, **f** 14 vol% low humidity

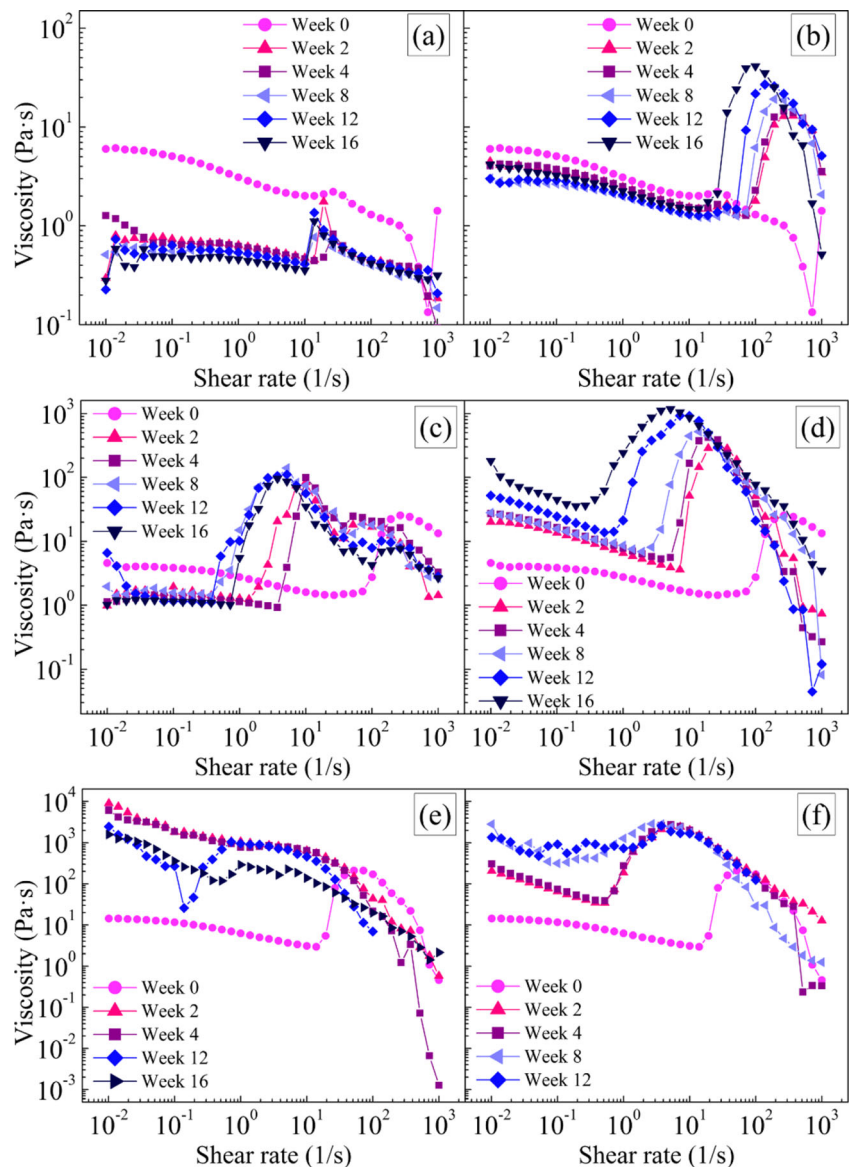


Table 7 Critical viscosity (η_c), viscosity increase ratio (η_c/η_{ons}), and critical shear rate ($\dot{\gamma}_c$) of the samples prepared with probe amplitude of 50% in the last week where they behaved as stable STFs (w_s)

Volume fraction of silica (%)	Regular humidity				Low humidity			
	w_s	η_c (Pa.s)	η_c/η_{ons}	$\dot{\gamma}_c$ (1/s)	w_s	η_c (Pa.s)	η_c/η_{ons}	$\dot{\gamma}_c$ (1/s)
10	16	1.11	3.96	13.90	16	41.22	27.90	26.80
12	16	95.61	94.43	1.00	16	1175.8	33.25	0.27
14	12	1050.2	40.76	0.14	12	2588.4	4.66	0.19

over time when stored in a dry environment. Even after 16 weeks, critical viscosity is still increasing. In contrast, the aging of the same sample in humid conditions promoted a considerable drop in overall viscosity and the maximum critical viscosity reached only around 1 Pa.s. A new aspect found in samples prepared with 50% of amplitude is that gelation did not occur in the sample containing 12% of silica over time, as shear thickening behavior persisted after 16 weeks. Even so, the viscosity at low shear rates increased progressively, indicating certain instability of this STF. Even more surprising is the fact that this sample can present shear thickening behavior in the presence of humidity. While samples stored in low humidity conditions have not reached a stable critical viscosity, samples in regular humidity environment reached an apparent stable condition past 4 weeks. The presence of water also reduced the viscosity of this sample at low shear rates, as seen in other situations, resulting in a high viscosity increase ratio of around 94. Samples with 14% of silica still did not remain stable. Shear thickening behavior persisted for up to 4 weeks, and the samples turned into a gel for longer aging times. Critical viscosity, viscosity increase ratio and critical shear rate of samples prepared using 50% of amplitude are shown in Table 7.

Based on these results, it is clear that water absorption is affecting the rheological behavior and stability of the STFs. The most obvious effect is that samples kept in a humid environment tend to have lower viscosities when compared to their dry counterparts. To further understand this issue, water uptake was analyzed by TGA. Tests were carried out in samples produced using 40% of amplitude to stipulate whether the absorption of water was affected by silica concentration. The results are shown in Table 8.

Water content was estimated by weight loss up to 125 °C, while silica content was estimated by the remaining weight at 550 °C, as there is little weight change above 500 °C. There was no significant difference in water content of samples with lower or higher amounts of silica. This means that neither PEG nor silica seem to be a preferable target for water to bond. Thus, lower viscosity in samples due to water absorption can possibly be explained by two reasons: first, STF showed to be very hygroscopic, absorbing around 13 wt.% of water after 16 weeks. As a result, a sample with an initial composition of 16.5 wt.% of silica (10 vol%) that absorbs 13% of water will decrease its silica concentration to 14.60 wt.% (8.6 vol%). This difference in composition leads to smaller viscosities and even loss of shear thickening behavior in samples close to the lower fraction limit, which is around 10 vol% of silica. A reduction of 1.4 vol% of particles represents a great difference in properties, as it was shown that changing 2 vol% causes a big impact in the shear thickening behavior from the different compositions studied. These results are in accordance with the study developed by Soutrenon et al. (2013).

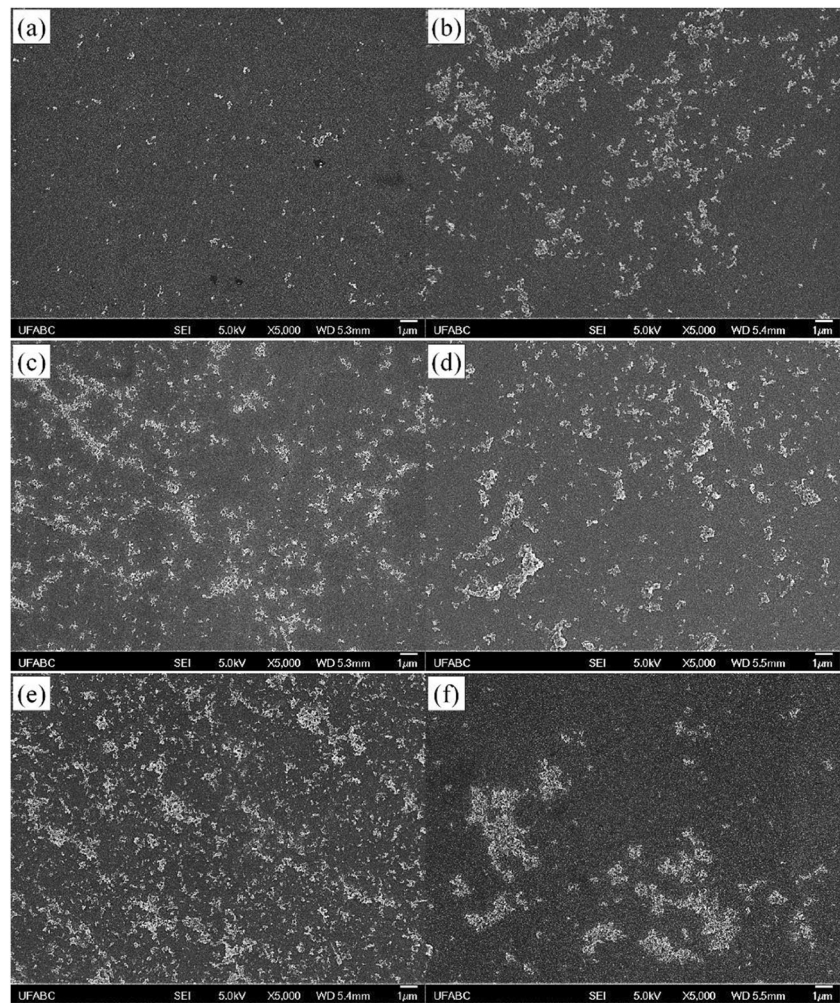
The second effect that water absorption causes to silica particles in STF is a reduction in agglomerate size. Water bonding to silica causes a reduction in hydroxyl groups available on the surface of the particles, hindering particle-particle bonding and agglomeration. A reduction in agglomerate size can also greatly reduce the shear thickening behavior (Barnes 1989; Gürgen et al. 2016; Chatterjee et al. 2019). Agglomeration reduction was confirmed by SEM images, shown in Fig. 5.

All three samples showed the presence of smaller agglomerates when stored in the presence of humidity. However, a decrease in the agglomeration of particles was mainly seen in samples with 10% of silica, where no big agglomerates are

Table 8 Water percentage after 4 months for samples prepared using 40% of amplitude and silica concentrations of 10 vol% (16.5 wt.%), 12 vol% (19.5 wt.%), and 14 vol% (22.5 wt.%)

Silica content (wt.%)	16.5		19.5		22.5	
	Regular	Low	Regular	Low	Regular	Low
Storage humidity						
Weight loss at 125 °C (%)	13.36	3.20	13.50	3.51	12.77	3.43
Remaining weight at 550 °C (%)	14.36	16.10	16.82	18.60	19.56	21.69

Fig. 5 SEM images of STF produced using 40% of amplitude after 16 weeks. **a** 10 vol% regular humidity, **b** 10 vol% low humidity, **c** 12 vol% regular humidity, **d** 12 vol% low humidity, **e** 14 vol% regular humidity, **f** 14 vol% low humidity



seen in Fig. 5a. These samples were also the only ones where the overall viscosity decreased over the weeks compared to initial tests, when stored in a regular humidity environment. Figure 6 summarizes the area distribution of particles from SEM images.

The area distribution shows that for all cases, samples stored in a low humidity environment show a much broader size distribution, whereas smaller agglomerates are predominant in samples stored in a regular humidity environment.

Table 9 summarizes the particle area average obtained from measurements from SEM images.

Another evidence of particle size reduction is a color change that happens in samples stored in a regular humidity environment, where they become blue, as seen in Fig. 7.

Studies have shown that suspensions of silica nanoparticles with sizes between 100 and 450 nm show a blue color caused by Rayleigh scattering (Ohsawa et al. 2002). Changes in color were seen for all sample compositions produced, indicating a higher amount of particles between 100 and 450 nm, which is

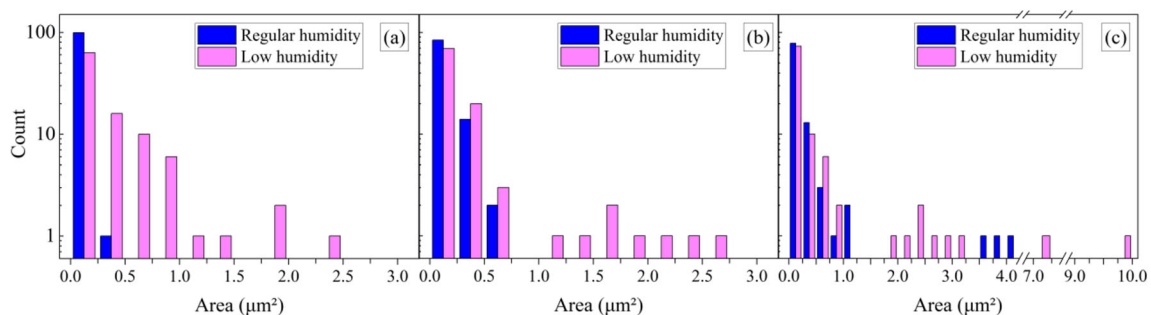


Fig. 6 Area distribution of agglomerates/aggregates from SEM images. **a** 10 vol.% of silica; **b** 12 vol.% of silica; **c** 14 vol.% of silica

Table 9 Average particle area of STF prepared with different silica content and stored in regular humidity or low humidity, measured from SEM images

Silica (vol.%)	Average particle area (μm^2)	
	Regular humidity	Low humidity
10	0.035 ± 0.04	0.348 ± 0.60
12	0.116 ± 0.13	0.303 ± 0.50
14	0.274 ± 0.66	0.490 ± 1.31

closer to the size of an aggregated particle of fumed silica (Barthel et al. 2008), indicating that part of these particles are no longer agglomerating, due to the presence of water.

The behavior of a typical STF sample over time, such as 12% of silica produced using 40% of probe amplitude is illustrated in Fig. 8. After dispersion, silica particles will agglomerate and flocculate when aging. When humidity is present, agglomerates will be smaller and there will be aggregate particles in the system.

As mentioned before, in the case of higher amounts of silica and/or smaller probe amplitudes, agglomerates will be bigger and form in shorter times. On the other hand, the agglomerates will be smaller for samples prepared with a smaller silica content and/or higher probe amplitudes, resulting in a deflocculated system that is stable for longer times, but with less prominent critical viscosity in week 0. In all cases aggregates will be formed when the STF is stored in room conditions, as evidenced by the blue coloring obtained for all samples not stored in a dry environment.

STF stability over shearing was also studied. Samples were tested for a total of 200 shearing cycles with a maximum shear rate of either 100 or 300 s^{-1} . Each shearing cycle lasted 5 s, followed by a resting cycle of 2 s at 0.1 s^{-1} . Viscosity as a function of shear rate was obtained before and after shearing in week 0 and week 4, as shown in Fig. 9 for samples produced using 40% of probe amplitude kept in dry conditions.

Shearing cycles reduce the critical viscosity and increase the critical shear rate of the samples. The higher the shear rate applied in the cycles, the higher is the damage to the shear thickening behavior. Samples with higher initial viscosity also exhibit the biggest viscosity reduction, as expected. Shearing can lead to agglomerate breakage, and higher viscosities in samples are caused by the presence of bigger agglomerates, being more susceptible to breaking. For 4-week-old samples, it is possible to see that the increase in viscosity occurred over time is not completely lost during shearing cycles. Still, there is a high decrease in properties, as this increase in viscosity is caused by particle agglomeration. DLS of samples before and after shearing was performed to measure average aggregate diameter, shown in Fig. 10.

When comparing the samples tested before any pre-shear, 4-week-old samples exhibit a broader particle diameter distribution, clearly showing that the particles increase in size over time, forming bigger agglomerates. Shearing cycles affect mostly the higher end of the distribution curve, indicating that shearing is not enough to break aggregates into primary particles, but only to reduce agglomerates to aggregates. The same behavior was seen in samples produced using 30 and 50% of probe amplitude, where shearing did not break agglomerates into primary particles. As helpful as DLS information is to measure quantitatively the size of particles in suspension, it is limited for further use because of the maximum particle size it can detect. The DLS equipment used does not provide reliable information for particles bigger than 1000 nm in diameter. Therefore, its use here is limited to analyzing and comparing the effect of shear on aggregates and primary particles of a certain size range, not being capable of measuring bigger agglomerates, as the ones seen by SEM. Tables 10 and 11 summarize the maximum viscosity after shearing of all compositions tested in week 0 and week 4, respectively.

Although at first sight, the initial viscosity magnitude seems to impact on the extent to which the viscosity will decrease when going through 200 shearing cycles, the dispersion energy and volume fraction of silica play a more

Fig. 7 Visual aspect of 10% silica-STF, produced using 40% of amplitude, after 16 weeks stored in **a** regular humidity; **b** low humidity

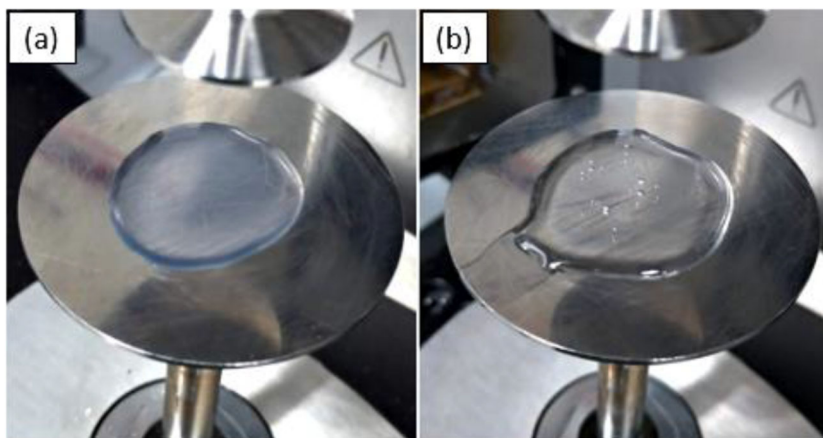


Fig. 8 Illustration of the influence of time and humidity on the general case of STFs composed of 12 vol% of silica produced with 40% of probe amplitude

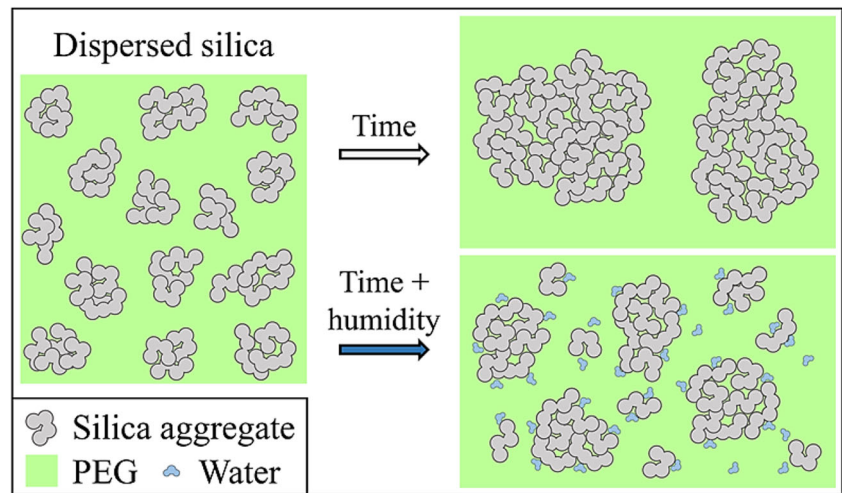


Fig. 9 Viscosity as a function of shear rate of samples with different silica content processed with 40% of probe amplitude, before shearing and after 200 cycles of shearing at a maximum shear rate of 100 and 300 s⁻¹. **a** 10 vol% week 0, **b** 10 vol% week 4, **c** 12 vol% week 0, **d** 12 vol% week 4, **e** 14 vol% week 0, **f** 14 vol% week 4

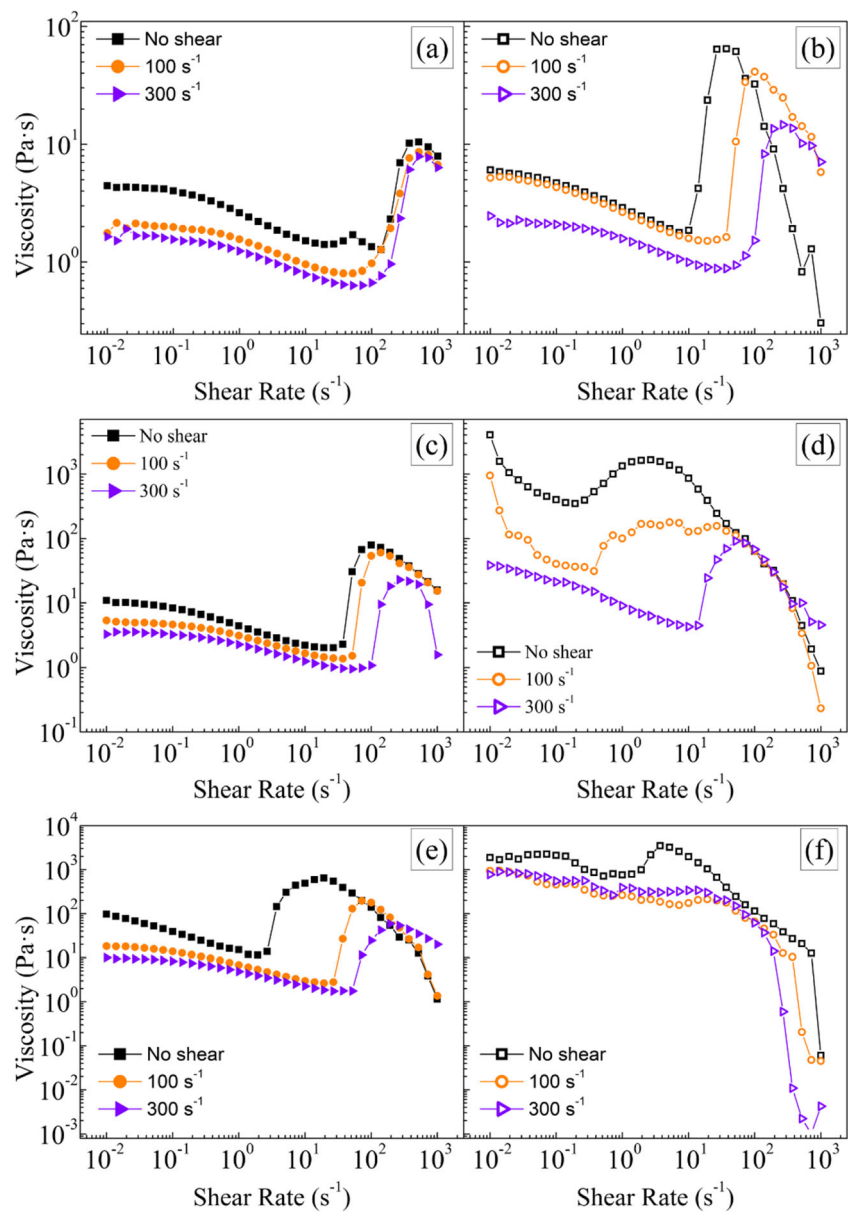
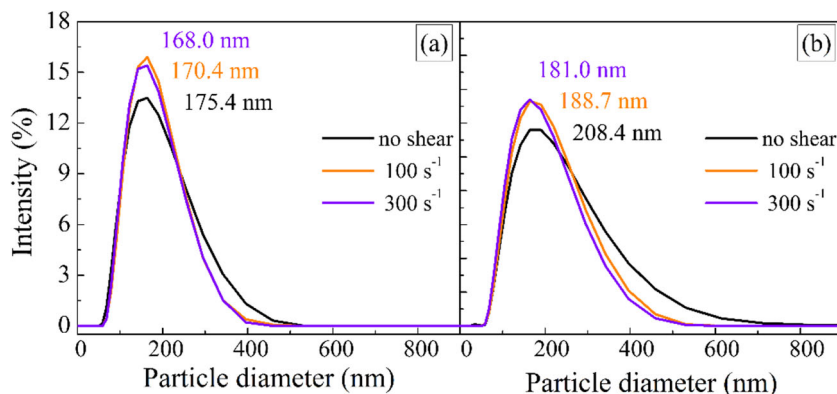


Fig. 10 Aggregate diameter distribution of samples with 10% of silica produced using 40% of probe amplitude, before and after 200 cycles of shearing at a maximum shear rate of 100 and 300 s⁻¹. **a** At week 0; **b** at week 4



important role in this loss. If we compare samples with similar critical viscosities, as in week 0, 10% of silica produced using 30% of amplitude and 12% of silica produced using 40% of amplitude, the first sample has a critical viscosity of 55.02 Pa.s, while the second one reaches 79.48 Pa.s. One would occasionally expect that the sample with a higher initial critical viscosity would display a higher decrease in viscosity, but what is seen is that the first sample exhibited a 47% loss in critical viscosity after the 100 s⁻¹ shearing cycles, while the second one lost only 24% under the same conditions. The same is seen for week 4 samples, taking for example the ones produced with 10% of silica using 30% of amplitude ($\eta_c = 757$ Pa.s) and 14% of silica produced with 50% of amplitude ($\eta_c = 1011.2$ Pa.s). The former lost 88.9% of its initial critical viscosity after 100 s⁻¹ shearing cycles, while the latter lost 83.4% under the same conditions, even though its initial critical viscosity is 33.5% higher. The main difference between these samples is that when using higher amplitudes (higher dispersion energy) to disperse silica, a higher particle volume fraction is required to obtain a similar critical viscosity, because the size of the agglomerates will be smaller due to higher dissipation energy. Both the volume fraction and size of particles present in a sample increase the critical viscosity of an STF (Barnes 1989), but only the size of the particles can be changed

during shearing, caused by the breakage of agglomerates, thus having a greater impact on the loss of properties of the STF.

Conclusions

STF stability was tested over time and over shearing for samples with 10, 12, and 14 vol% of A200 fumed silica in PEG 300, dispersed using ultrasonication probe amplitude of 30, 40, and 50%. Increasing the amount of silica or decreasing probe amplitude resulted in higher viscosities, but it also led to faster destabilization of the STF over time. When samples were stored in the presence of humidity, their overall viscosity was smaller than for the samples kept in a low humidity environment, but in both cases samples became a gel if using higher amounts of silica or dispersing using smaller probe amplitudes. Silica was found to agglomerate over time, resulting in flocculated systems, while water reduced this tendency to agglomerate, decreasing viscosity. Samples with smaller amounts of silica or produced using higher dispersion energy did not become gels, but a viscosity increase over time was observed when stored in low humidity conditions. The sample with 12 vol% of silica produced with 50% of probe

Table 10 Critical viscosity (η_c) and critical shear rate ($\dot{\gamma}_c$) for fresh samples (week 0) before and after 200 cycles of shearing at a maximum shear rate of 100 and 300 s⁻¹. Numbers in parentheses indicate the viscosity increase ratio (η_c/η_{0ns})

Week 0		No shear		100 s ⁻¹		300 s ⁻¹	
Probe amplitude (%)	Silica (vol%)	η_c (Pa.s) (η_c/η_{0ns})	$\dot{\gamma}_c$ (1/s)	η_c (Pa.s) (η_c/η_{0ns})	$\dot{\gamma}_c$ (1/s)	η_c (Pa.s) (η_c/η_{0ns})	$\dot{\gamma}_c$ (1/s)
30	10	55.02 (36.57)	26.8	29.17 (29.69)	51.8	13.42 (17.27)	139
	12	519.3 (93.69)	3.73	76.14 (55.22)	51.8	32.08 (30.51)	100
	14	3979.6 (5.13)	1.00	476.2 (4.12)	10	82.29 (37.15)	37.3
40	10	10.44 (8.20)	193	8.62 (10.75)	72	7.89 (12.45)	100
	12	79.48 (39.19)	26.8	60.42 (44.03)	51.8	22.9 (24.02)	72
	14	643.04 (56.19)	2.68	196.27 (74.32)	26.8	58.68 (33.41)	72
50	10	—	—	—	—	—	—
	12	23.48 (15.68)	139	21.08 (20.30)	139	18.07 (20.63)	139
	14	184.11 (67.21)	37.3	74.26 (47.15)	72	38.75 (30.94)	100

Table 11 Critical viscosity (η_c) and critical shear rate ($\dot{\gamma}_c$) for 4-week-old samples before and after 200 cycles of shearing at a maximum shear rate of 100 and 300 s⁻¹. Numbers in parentheses indicate the viscosity increase ratio (η_c/η_{ons})

Week 4		No shear		100 s ⁻¹		300 s ⁻¹	
Probe amplitude (%)	Silica (vol%)	η_c (Pa.s) (η_c/η_{ons})	Critical shear rate (1/s)	η_c (Pa.s) (η_c/η_{ons})	Critical shear rate (1/s)	η_c (Pa.s) (η_c/η_{ons})	Critical shear rate (1/s)
30	10	757.3 (54.13)	0.72	84.1 (24.13)	7.2	29.28 (23.21)	72
	12	–	–	233.02 (8.01)	5.18	105.9 (14.53)	5.18
	14	–	–	–	–	–	–
40	10	64.56 (36.16)	10	41.20 (27.24)	26.8	14.67 (16.64)	37.3
	12	1667.4 (4.75)	0.193	178.69 (5.40)	0.37	91.12 (21.12)	51.8
	14	2253.1 (4.89)	1.93	–	–	–	–
50	10	7.15 (7.19)	268	5.75 (8.47)	518	7.74 (11.92)	139
	12	209.37 (70.00)	10	77.55 (37.26)	37.3	30.898 (25.11)	51.8
	14	1011.2 (2.89)	0.37	168.21 (19.27)	26.8	124.55 (34.66)	37.3

amplitude was the only one that showed a significant magnitude of discontinuous shear thickening when stored in a regular humidity environment, balancing the effects of agglomeration over time and agglomerate breakage due to humidity. Considering that for potential impact-absorbing applications STFs are expected to remain stable over time and they should also keep their properties after indefinite mechanical loading cycles, we tested the influence of pre-shearing cycles on the stability of shear thickening behavior. High shear rate cycles were found to promote agglomerate breakage to different extents, depending on STF composition and processing conditions. This effect was more prominent in samples containing lower amounts of silica produced using low dispersion energy. Such samples initially exhibited shear thickening behavior due to the presence of big agglomerates, but these are more prone to breakage under shear, so the STF properties are degraded after a series of shearing cycles.

Acknowledgments The authors acknowledge the Multiuser Central Facilities (CEM) at UFABC for the use of SEM and DLS and CAPES for financial support.

Funding information This work was supported by Coordenação de Aperfeiçoamento de Pessoal de Nível Superior–Brasil (CAPES)–Finance Code 001, for the master’s scholarship of D. A. H.

Compliance with ethical standards

Conflict of interest The authors declare that they have no conflict of interest.

References

Barnes HA (1989) Shear-thickening (“Dilatancy”) in suspensions of nonaggregating solid particles dispersed in Newtonian liquids. *J Rheol* (N Y N Y) 33:329–366. <https://doi.org/10.1122/1.550017>

- Barthel H, Rösch L, Weis J (2008) Fumed silica - production, properties, and applications. *Organosilicon Chem I Mol Mater*:761–778. <https://doi.org/10.1002/9783527620777.ch91a>
- Bertrand E, Bibette J, Schmitt V (2002) From shear thickening to shear-induced jamming. *Phys Rev E Stat Nonlin Soft Matter Phys* 66:060401. <https://doi.org/10.1103/PhysRevE.66.060401>
- Birkin PR, Offin DG, Joseph PF, Leighton TG (2005) Cavitation, shock waves and the invasive nature of sonoelectrochemistry. *J Phys Chem B* 109:16997–17005. <https://doi.org/10.1021/jp051619w>
- Blees MH (2002) Foundations of colloid science. *Colloids Surf A Physicochem Eng Asp* 210:125. [https://doi.org/10.1016/S0927-7757\(02\)00170-x](https://doi.org/10.1016/S0927-7757(02)00170-x)
- Bossis G (1985) The rheology of concentrated suspensions of spheres in simple shear flow by numerical simulation. *J Fluid Mech* 155:105. <https://doi.org/10.1017/S0022112085001732>
- Brown E, Forman NA, Orellana CS, Zhang H, Maynor BW, Betts DE, DeSimone JM, Jaeger HM (2010) Generality of shear thickening in dense suspensions. *Nat Mater* 9:220–224. <https://doi.org/10.1038/nmat2627>
- Brown E, Jaeger HM (2012) The role of dilation and confining stresses in shear thickening of dense suspensions. *J Rheol* 56:875–923. <https://doi.org/10.1122/1.4709423>
- Cao S, He Q, Pang H, Chen K, Jiang W, Gong X (2018) Stress relaxation in the transition from shear thinning to shear jamming in shear thickening fluid. *Smart Mater Struct* 27:085013. <https://doi.org/10.1088/1361-665X/aacb8>
- Chatterjee VA, Dey P, Verma SK, Bhattacharjee D, Biswas I, Neogi S (2019) Probing the intensity of dilatancy of high performance shear-thickening fluids comprising silica in polyethylene glycol. *Mater Res Express* 6. <https://doi.org/10.1088/2053-1591/ab1185>
- Egges RG, Halbach CJ, Decker MJ, et al (2005) Stab performance of shear thickening fluid (STF)-fabric composites for body armor applications. In: *International SAMPE Symposium and Exhibition (Proceedings)*
- Feng X, Li S, Wang Y, Wang Y, Liu J (2014) Effects of different silica particles on quasi-static stab resistant properties of fabrics impregnated with shear thickening fluids. *Mater Des* 64:456–461. <https://doi.org/10.1016/j.matdes.2014.06.060>
- Freundlich H, Jones AD (1936) Sedimentation volume, dilatancy, thixotropic and plastic properties of concentrated suspensions. *J Phys Chem* 40:1217–1236. <https://doi.org/10.1021/j150378a012>
- Gedanken A (2003) Sonochemistry and its application to nanochemistry. *Curr Sci* 85:1720

- Gürgen S, Kuşhan MC (2017) The stab resistance of fabrics impregnated with shear thickening fluids including various particle size of additives. *Compos Part A Appl Sci Manuf* 94:50–60. <https://doi.org/10.1016/j.compositesa.2016.12.019>
- Gürgen S, Li W, Kuşhan MC (2016) The rheology of shear thickening fluids with various ceramic particle additives. *Mater Des* 104:312–319. <https://doi.org/10.1016/j.matdes.2016.05.055>
- Hoffman RL (1974) Discontinuous and dilatant viscosity behavior in concentrated suspensions. II Theory and experimental tests. *J Colloid Interface Sci* 46:491–506. [https://doi.org/10.1016/0021-9797\(74\)90059-9](https://doi.org/10.1016/0021-9797(74)90059-9)
- Hoffman RL (1972) Discontinuous and dilatant viscosity behavior in concentrated suspensions. *J Rheol* 114:10514–10527. <https://doi.org/10.1063/1.1373687>
- Hoffman RL (1982) Discontinuous and dilatant viscosity behavior in concentrated suspensions III. Necessary conditions for their occurrence in viscometric flows. *Adv Colloid Interface Sci* 17:161–184. [https://doi.org/10.1016/0001-8686\(82\)80017-1](https://doi.org/10.1016/0001-8686(82)80017-1)
- Hoffman RL (1998) Explanations for the cause of shear thickening in concentrated colloidal suspensions. *J Rheol* 42:111–123. <https://doi.org/10.1122/1.550884>
- Hunter RJ (2001) *Foundations of colloid science* (2nd edition)
- Khalili F, De Paoli F, Guldiken R (2015) Impact resistance of liquid body armor utilizing shear thickening fluids: a computational study. In: *ASME International Mechanical Engineering Congress and Exposition, Proceedings (IMECE)*
- Laskowski J, Kitchener JA (1969) The hydrophilic-hydrophobic transition on silica. *J Colloid Interface Sci* 29:670–679. [https://doi.org/10.1016/0021-9797\(69\)90219-7](https://doi.org/10.1016/0021-9797(69)90219-7)
- Lee YS, Wetzel ED, Wagner NJ (2003) The ballistic impact characteristics of Kevlar® woven fabrics impregnated with a colloidal shear thickening fluid. *J Mater Sci* 38:2825–2833. <https://doi.org/10.1023/A:1024424200221>
- Liu XQ, Bao RY, Wu XJ, Yang W, Xie BH, Yang MB (2015) Temperature induced gelation transition of a fumed silica/PEG shear thickening fluid. *RSC Adv* 5:18367–18374. <https://doi.org/10.1039/c4ra16261g>
- Maranzano BJ, Wagner NJ (2001) The effects of particle size on reversible shear thickening of concentrated colloidal dispersions. *J Chem Phys* 114:10514–10527. <https://doi.org/10.1063/1.1373687>
- Metzner AB, Whitlock M (1958) Flow behavior of concentrated (dilatant) suspensions. *Trans Soc Rheol* 2:239–254. <https://doi.org/10.1122/1.548831>
- Mewis J, Wagner NJ (2012) *Colloidal suspension rheology*. Cambridge University Press, Cambridge
- Negi AS, Osuji CO (2009) New insights on fumed colloidal rheology - shear thickening and vorticity-aligned structures in flocculating dispersions. In: *Rheologica Acta*
- Ohsawa S, Kawamura T, Takamatsu N, Yusa Y (2002) Rayleigh scattering by aqueous colloidal silica as a cause for the blue color of hydrothermal water. *J Volcanol Geotherm Res* 113:49–60. [https://doi.org/10.1016/S0377-0273\(01\)00250-5](https://doi.org/10.1016/S0377-0273(01)00250-5)
- Raghavan SR, Khan SA (1997) Shear-thickening response of fumed silica suspensions under steady and oscillatory shear. *J Colloid Interface Sci* 185:57–67. <https://doi.org/10.1006/jcis.1996.4581>
- Raghavan SR, Walls HJ, Khan SA (2000) Rheology of silica dispersions in organic liquids: new evidence for solvation forces dictated by hydrogen bonding. *Langmuir*. 16:7920–7930. <https://doi.org/10.1021/la991548q>
- Reynolds O (1885) LVII. On the dilatancy of media composed of rigid particles in contact. With experimental illustrations. *London, Edinburgh, Dublin Philos Mag J Sci* 20:469. <https://doi.org/10.1080/14786448508627791>
- Singh M, Verma SK, Biswas I, Mehta R (2019) Rheology of fumed silica and polyethylene glycol shear thickening suspension with nano-clay as an additive. *J Polym Eng* 39:48–57. <https://doi.org/10.1515/polyeng-2018-0054>
- Song Z, Zhang C, Song M, Wu S (2011) Advanced stab resistance fabrics utilizing shear thickening fluids. In: *Advanced Materials Research*
- Soutrenon M, Michaud V, Manson JAE (2013) Influence of processing and storage on the shear thickening properties of highly concentrated monodisperse silica particles in polyethylene glycol. *Appl Rheol* 23. <https://doi.org/10.3933/ApplRheol-23-54865>
- Taurozzi JS, Hackley VA, Wiesner MR (2011) Ultrasonic dispersion of nanoparticles for environmental, health and safety assessment issues and recommendations. *Nanotoxicology*. 5:711–729. <https://doi.org/10.3109/17435390.2010.528846>
- Warren J, Offenberger S, Toghiani H, Pittman CU Jr, Lacy TE, Kundu S (2015) Effect of temperature on the shear-thickening behavior of Fumed silica suspensions. *ACS Appl Mater Interfaces* 7:18650–18661. <https://doi.org/10.1021/acsami.5b05094>
- Lee YS, Wetzel ED, Egres RG Jr, Wagner NJ (2013) Advanced body armor utilizing shear thickening fluids. *J Chem Inf Model*. <https://doi.org/10.1017/CBO9781107415324.004>

Publisher's note Springer Nature remains neutral with regard to jurisdictional claims in published maps and institutional affiliations.